International Journal of Mass Spectrometry 314 (2012) 6–12

Contents lists available at SciVerse ScienceDirect

International Journal of Mass Spectrometry

journal homepage: www.elsevier.com/locate/ijms

# A study of octupolar excitation for mass-selective centering in Penning traps

M. Rosenbusch[a,*], Ch. Böhm[b], Ch. Borgmann[b], M. Breitenfeldt[c], A. Herlert[d], M. Kowalska[d], S. Kreim[b], G. Marx[a], S. Naimi[e], D. Neidherr[b], R. Schneider[a], L. Schweikhard[a]

[a] Ernst-Moritz-Arndt-Universität Greifswald, 17487 Greifswald, Germany
[b] Max-Planck-Institut für Kernphysik, 69117 Heidelberg, Germany
[c] Katholieke Universiteit Leuven, 3000 Leuven, Belgium
[d] CERN, 1211 Geneva 23, Switzerland
[e] CSNSM-IN2P3-CNRS, 91405 Orsay-Campus, France

ARTICLE INFO

*Article history:*
Received 20 September 2011
Received in revised form 5 January 2012
Accepted 6 January 2012
Available online 17 January 2012

*Keywords:*
Penning trap
Octupolar excitation
Mass-selective ion centering

ABSTRACT

Octupolar excitation has been investigated with respect to mass-selective ion centering in buffer-gas filled Penning traps for the isolation of an ion species of interest. To this end, off-line test measurements have been performed with the preparation Penning trap of the mass spectrometer ISOLTRAP located at ISOLDE/CERN including a comparison with the conventional quadrupolar excitation. The experimental results are compared to numerical simulations of ions under influence of quadrupolar and octupolar excitation.



## 1. Introduction

The combined application of quadrupolar excitation and buffer-gas cooling of the ion motion is a well-established method for mass-selective ion centering in Penning traps. After its introduction at ISOLTRAP [1] as a preparatory step for precision mass spectrometry of short-lived radionuclei [2,3], the method has quickly been transferred [4] to (Fourier transform) ion cyclotron resonance (FT-ICR) cells. In analytical chemistry applications it is often implemented as part of the standard procedure of complex event sequences, either for axialization of particular species [5] or broader ranges of mass-over-charge ratios [6].

In particular in the case of the Penning trap application for nuclear mass spectrometry, the purification of the ensemble of ions of interest from isobars or isomers delivered at the same time, is a key element in securing the accuracy of the resulting mass values. The "quadrupolar cooling" has become the method of choice to separate the ion species reaching resolving powers of typically $R = m/\Delta m = 10^4$–$10^5$. Many species of interest require even higher resolving powers for the separation from contaminants [7]. Resolving powers of several $10^5$ can be reached by use of dipolar excitation for radial ion ejection in buffer-gas free Penning traps [8]. In addition, the "Ramsey excitation scheme" of time-separated oscillatory fields [9,10] has been applied for ion separation [11]. The duration of these processes is mostly on the order of a second. Thus, for very short-lived nuclides other methods are needed. In the following, a new approach for the improvement of the cooling process is studied. It is based on the replacement of the quadrupolar excitation by an octupolar excitation, which has recently been introduced to ion-cyclotron-resonance mass spectrometry [12–15].

A short review of octupolar excitation in vacuum is given followed by the introduction of a damping force in the context of quadrupolar excitation. The latter is a well-studied scheme for which the most important parameters and their influences are discussed. The experimental results for quadrupolar and octupolar excitation are reviewed with respect to centering efficiency and resolving power. In addition, both buffer-gas cooling schemes are studied with simulations using a binary-collision model, which agrees with the experimental findings.

## 2. Octupolar excitation

A major motivation for the introduction of octupolar excitation to Penning-trap mass spectrometry was the doubling of the resonance frequency for the conversion of the radial motional modes as compared to quadrupolar excitation, namely from $\nu_c$ to $2\nu_c$, where $\nu_c$ is the cyclotron frequency $\nu_c = qB/(2\pi m) = \omega_c/2\pi$, which is for an ideal trap the sum of the radial eigenfrequencies $\nu_c = \nu_+ + \nu_-$ (cyclotron motion with reduced cyclotron frequency $\nu_+ = \omega_+/2\pi$ and magnetron motion with magnetron frequency $\nu_- = \omega_-/2\pi$ of

* Corresponding author.
*E-mail address:* marco.rosenbusch@cern.ch (M. Rosenbusch).

1387-3806/$ – see front matter © 2012 Elsevier B.V. All rights reserved.
doi:10.1016/j.ijms.2012.01.002

a charged particle in the Penning-trap). Here the magnetic field strength is denoted by $B$; $m$ and $q$ are the mass and the charge of the trapped ion, respectively. For the motional modes and eigenfrequencies of ions in Penning traps see Refs. [16,17]. The hope of obtaining a similar resonance width, and thus an increase by a factor of two in mass precision, triggered the interest in the application for high-precision mass spectrometry of short-lived nuclei. Even higher resolving powers have been found due to the non-linear nature of octupolar excitation [12,13].

The octupolar excitation field as a function of the excitation time $\tau$ can be written in the form [12]

$$\begin{aligned} E_x(\tau) &= (x^3 - 3xy^2)\frac{4U_{\mathrm{oct}}}{a^4}\cos(\omega_{\mathrm{oct}}\tau + \varphi_{\mathrm{oct}}(0)), \\ E_y(\tau) &= (y^3 - 3x^2y)\frac{4U_{\mathrm{oct}}}{a^4}\cos(\omega_{\mathrm{oct}}\tau + \varphi_{\mathrm{oct}}(0)), \end{aligned} \tag{1}$$

where $U_{\mathrm{oct}}$ is the excitation amplitude defining the maximum potential on a circle with the radius $a$, $\omega_{\mathrm{oct}} = 2\pi\nu_{\mathrm{oct}}$ the angular frequency of octupolar excitation, and $\varphi_{\mathrm{oct}}(0)$ the starting phase of the external octupolar field. The radial equations of motion of an ion in a Penning trap can be written conveniently when the coordinates $\vec{\rho} = (x, y)$ are substituted [16] by

$$\vec{V}^{\pm} = \dot{\vec{\rho}} - \omega_{\mp}\hat{z} \times \vec{\rho}, \tag{2}$$

where $\hat{z}$ is the unit vector in axial direction. Thus, the equation of motion of a single ion in the presence of octupolar excitation is obtained as

$$\begin{aligned} \dot{V}_x^{\pm} &= -\omega_{\pm}V_y^{\pm} + G_{\mathrm{oct}}\left(V_y^{+} - V_y^{-}\right)\left[\left(V_y^{+} - V_y^{-}\right)^2 - 3\left(V_x^{+} - V_x^{-}\right)^2\right] \\ \dot{V}_y^{\pm} &= -\omega_{\pm}V_x^{\pm} + G_{\mathrm{oct}}\left(V_x^{+} - V_x^{-}\right)\left[\left(V_x^{+} - V_x^{-}\right)^2 - 3\left(V_y^{+} - V_y^{-}\right)^2\right] \end{aligned} \tag{3}$$

with the oscillation term

$$G_{\mathrm{oct}} = g_{\mathrm{oct}}\cos(\omega_{\mathrm{oct}}\tau + \varphi_{\mathrm{oct}}(0)), \tag{4}$$

and the coupling parameter

$$g_{\mathrm{oct}} = \frac{q}{m}\frac{4U_{\mathrm{oct}}}{a^4(\omega_{+} - \omega_{-})^3} \tag{5}$$

An analytical solution of the equation of motion, Eq. (3), has been worked out recently [15].

The resolving power of octupolar resonances is expected to be up to more than two orders of magnitude higher than for quadrupolar excitation under ideal conditions (i.e., 200 times higher [12]), an improvement of only an order of magnitude has so far been demonstrated in experiments [12,13,15]. In contrast to the case of quadrupolar excitation, the ion motion under octupolar excitation depends very sensitively on the initial conditions (position and velocity of the ion). The quality of a resonance can be affected, e.g., due to the dependency of the conversion duration on the initial radius leading to asynchronous conversions of ions in an expanded cloud. In a buffer-gas environment, collisions are expected to further influence the ion motion and thus to degrade the resonance shapes and to increase their widths. In order to study whether buffer-gas cooling can be improved by using octupolar instead of quadrupolar excitation, experimental and simulation studies have been performed which are described in the following.

## 3. Characteristic parameters of the cooling process

Since the quadrupolar excitation including a damping force has already been described [18,19], it will now be used to introduce and discuss the influence of the parameters on the cooling process. As opposed to an excitation in vacuum, where excitation duration and amplitude are the main parameters, collisions with the buffer gas now enter into the equation of motion as a damping-force,

$$\vec{F} = -2m\gamma\vec{v}, \tag{6}$$

where $\gamma$ is the damping coefficient and $\vec{v}$ the velocity of the ion. The damping coefficient is connected by

$$2m\gamma = \frac{q}{K} \tag{7}$$

to the ion mobility $K$, which depends on the pressure $p$ and temperature of the buffer gas, and the corresponding ion-atom collision cross-section [20].

The principle of mass-selective centering consists of two simultaneous processes. A quadrupolar excitation (excitation frequency $\nu_{\mathrm{q}}$) at $\nu_{\mathrm{q}} = \nu_c$ results in a conversion of an initially pure magnetron motion into cyclotron motion [21]. Secondly, the cyclotron motion is cooled by the buffer gas. Thus, the resonantly excited ions move to the trap center while the ions that are not on resonance remain on their magnetron orbits which is even further increased by the buffer-gas collisions [1]. Mass selection is achieved when the ions of interest are axially ejected through a central opening, whereas the others, which have not been centered, are blocked by the endcap electrodes (see also Section 4).

An analytical solution of the ion motion in the presence of a quadrupolar excitation and a damping force can be found in Ref. [19]. The cooling process is described by analysing the magnetron motion. To this end the ratio $f_M = f_M(\delta, \tau, g_{\mathrm{q}}, \gamma) = \rho_{-}(\tau)/\rho_{-}(0)$ of the magnetron radius $\rho_{-}(\tau)$ at time $\tau$ to its initial value $\rho_{-}(0)$ is defined in analogy to Eq. (26) in Ref. [19]. Parameters are the damping coefficient $\gamma$, the detuning $\delta = \omega_{\mathrm{q}} - \omega_c = 2\pi(\nu_{\mathrm{q}} - \nu_c)$ of the excitation frequency $\nu_{\mathrm{q}}$ from the resonance frequency $\nu_c$, and the coupling factor $g_{\mathrm{q}}$ of the quadrupolar excitation

$$g_{\mathrm{q}} = \frac{q}{m}\frac{2U_{\mathrm{q}}}{a^2(\omega_{+} - \omega_{-})}, \tag{8}$$

which depends on the quadrupolar excitation amplitude $U_{\mathrm{q}}$ and the parameter $a$ (defined in analogy to the corresponding parameters $U_{\mathrm{oct}}$ and $a$ of Eq. (5)).

For the initial condition of zero cyclotron radius $\rho_{+}(0) = 0$, the ratio $f_{\mathrm{M}}$ is given by

$$f_{\mathrm{M}}(\delta, \tau, g_{\mathrm{q}}, \gamma) = \frac{\rho_{-}(\tau)}{\rho_{-}(0)} = e^{-\gamma\tau}\xi\xi^{*}, \tag{9}$$

where

$$\xi = \sqrt{\cos\frac{\overline{\omega}_R\tau}{2} - \mathrm{i}\frac{\delta + \mathrm{i}\widetilde{\gamma}_1(\gamma)}{\overline{\omega}_R}\sin\frac{\overline{\omega}_R\tau}{2}} \tag{10}$$

and $\xi^{*}$ is the complex conjugate of $\xi$. The modified Rabi frequency $\overline{\omega}_R = \overline{\omega}_R(\delta, g_{\mathrm{q}}, \gamma)$ of the conversion of the motional modes with damping is given by

$$\overline{\omega}_R(\delta, g_{\mathrm{q}}, \gamma) = \sqrt{4g_{\mathrm{q}}^2 + \delta^2 - \widetilde{\gamma}_1(\gamma)^2 + 2\mathrm{i}\delta\widetilde{\gamma}_1(\gamma)}. \tag{11}$$

A first order approximation of $\widetilde{\gamma}_1$ (Eq. (19) of [19]) leads to

$$\widetilde{\gamma}_1(\gamma) = 2\gamma\frac{\omega_c}{\omega_1} \tag{12}$$

with

$$\omega_1 = \sqrt{\omega_c^2 - 2\omega_z^2}, \tag{13}$$

where $\omega_z$ is the frequency of the axial ion oscillation.

### 3.1. Resonant excitation including a damping force

The variation of the damping coefficient $\gamma$ versus the coupling factor $g_{\mathrm{q}}$ creates different cases of ion motion for resonantly excited

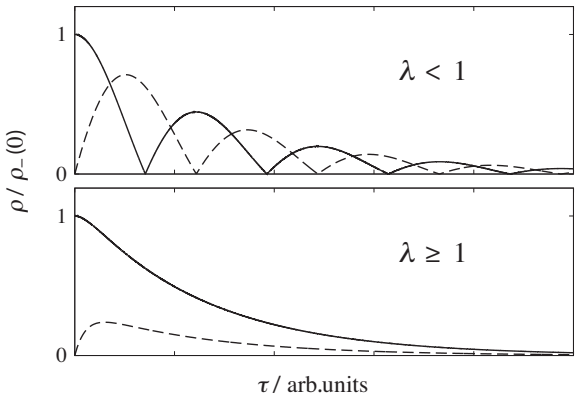


**Fig. 1.** Magnetron (solid line), and cyclotron radius (dashed line), as a function of the excitation time $\tau$ for quadrupolar on-resonance excitation under different damping conditions, $\lambda < 1$ (top) and $\lambda \geq 1$ (bottom).

ions [18]. It is convenient to normalize the damping coefficient with a scaling parameter $\lambda$

$$\gamma(\lambda) = g_q \frac{\omega_1}{\omega_c}\lambda. \tag{14}$$

A weak damping, namely $\lambda < 1$ and thus $\gamma < g_q(\omega_1/\omega_c)$, leads to an oscillating-motion scheme due to a real $\overline{\omega}_R$. During the excitation, the ions are approaching the trap center while the cyclotron and magnetron mode are converted back and forth into each other (see Fig. 1, top). For $\lambda \geq 1$, $\overline{\omega}_R$ is imaginary and the magnetron motion is decreasing exponentially (Fig. 1, bottom) in analogy to the overdamped motion of a harmonic oscillator. In order to center the ions, the parameter $\lambda$ may not exceed $\omega_c/(\sqrt{2}\omega_z)$ [18]. Otherwise, the damping coefficient $\gamma$ is too large for the applied coupling factor $g_q$ and the magnetron radius cannot be decreased or, for an even larger $\lambda$, increases during the excitation.

### 3.2. Resolving power for ion centering with damping

Fig. 2 shows the magnetron radius $\rho_-$ after quadrupolar excitation (excitation duration $\tau_0$) as a function of the normalized frequency detuning $\delta/2\pi\tau_0$ and normalized to the initial magnetron radius $\rho_-(0)$. The scaling parameter $\lambda$ has been varied as $\lambda = 1/10$ (dotted line), $\lambda = 1/2$ (dashed line), and $\lambda = 1$ (solid line). The width of the resonance curve is increasing with the parameter $\lambda$ leading

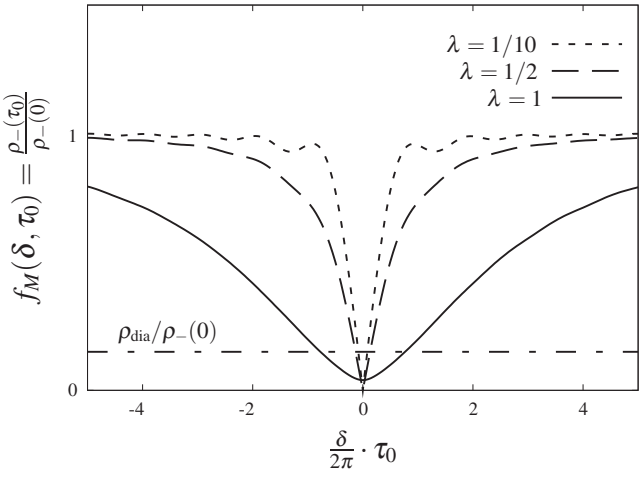


**Fig. 2.** $f_M(\delta, \tau_0)$ as a function of the normalized frequency detuning $\delta/2\pi\tau_0$. Straight line at the bottom: radius $\rho_{dia}$ of the ejection hole of the Penning trap (see also Section 4).

as expected to high resolving powers $R = \Delta\nu_{mag}/\nu_c$ at low pressures, where $\Delta\nu_{mag}$ is the FWHM of each curve. For the oscillating-motion scheme ($\lambda = 1/10$ and $1/2$), the coupling factor $g_q$ is chosen such that only the first complete conversion is performed, leading to the highest resolving power. This corresponds to

$$g_q = g_{q_{min}} = \frac{\arccos(-\lambda)}{\sqrt{1-\lambda^2}\tau_0}. \tag{15}$$

For the overdamped scheme ($\lambda = 1$) the coupling factor $g_{q_{min}}$ does not exist, since no complete conversions are carried out. In this case the amplitude should be chosen sufficiently small to keep the centering effect on off-resonantly excited ions low but still large enough to center and eject the ions of interest after cooling the cyclotron radius.

By use of the dimensionless expression $\delta/(2\pi)\tau_0$ the resonance curves are independent of the excitation duration $\tau_0$, thus providing a common approach for the high-vacuum case [18]. For a non-zero damping coefficient $\gamma$ this is no longer valid. This is why the parameter $\lambda$ has been introduced. For a given $\lambda$, the coupling factor $g_{q_{min}}$ is proportional to $1/\tau_0$. This causes an elimination of $\tau = \tau_0$ in Eq. (9) if $\delta$ is normalized to $\tau_0$. Also for the overdamped scheme the dependency of $g_q \propto 1/\tau_0$ holds if the final conversion degree is constant ($\rho_-(\tau_0)$ fixed).

## 4. Experimental setup and procedure

The experimental investigations have been performed in the preparation Penning trap of ISOLTRAP [22] (Fig. 3 top). Singly charged cesium ions ($^{133}Cs^+$) are delivered from a surface-ionization ion source and are accumulated in a RFQ buncher [22,23]. The cylindrical Penning trap is located in the bore of a superconducting magnet with a field strength of 4.7 T. The ring electrode has eight segments, which allows the application of an octupolar radio-frequency (rf) field. The inner diameter of the trap is 20 mm which ensures a good acceptance of ions which are slowly injected using retardation electrodes. A diaphragm with a diameter of $\rho_{dia} = 3$ mm is placed at the upper end of the trap realizing the radial selection of ions and serving as a pumping barrier towards the upper part of the setup [22]. A microchannel-plate (MCP) detector is located about 1 m above the trap and the ion-optical elements between the trap and the detector have been optimized for ions starting from the trap axes. A pressure of $p = 10^{-5}$ mbar up to several times $10^{-4}$ mbar inside the buffer-gas filled Penning trap is estimated from measurements with a Penning gauge located about 1 m below the trap, where the pressure $p_{read}$ is about two orders of magnitude lower.

The time structure of the experimental cycle is shown in the bottom of Fig. 3. The ion bunch is captured in the preparation Penning trap by lowering the voltage at the lower endcap (capture pulse *A*). After a waiting time (*B*) to cool the axial oscillation of the ion motion the radial rf-signals are applied to the ring segments (*C*–*F*). First, a quadrupolar excitation at the resonance frequency $\nu_c$ of the cesium ions is applied (*C*) for radial centering. A waiting time for radial cooling (*D*) is implemented to decrease the remaining cyclotron radius after this excitation. These two steps have been added to the standard sequence for the study comparing the effect of quadrupolar and octupolar excitation. They are usually not applied during on-line investigations of short-lived nuclides. Subsequently, all ions are excited by a dipolar rf-signal (*E*) at the magnetron frequency $\nu_-$ to achieve an average magnetron radius of typically 4–7 mm depending on the strength of the excitation. This is followed by the main centering excitation (*F*) which is the focus of the present work: either a quadrupolar excitation around $\nu_c$ or an octupolar excitation around $2\nu_c$ indicated by the dashed lines in Fig. 3 bottom. After a second radial-cooling time (*G*), an extraction pulse (*H*) ejects the centered ions towards the detector.

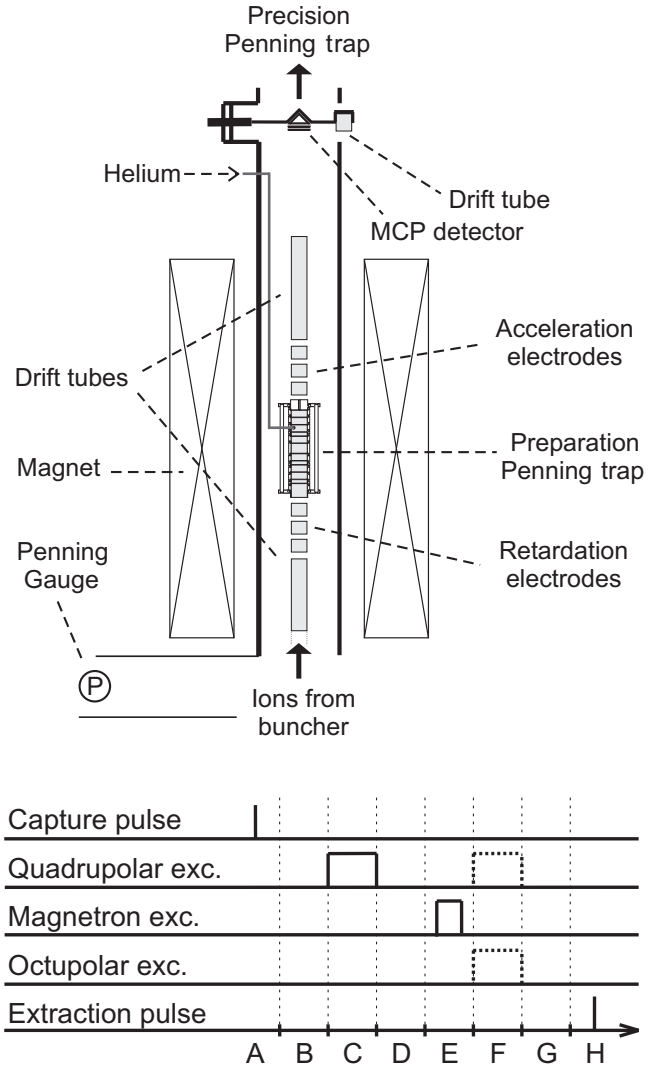


**Fig. 3.** Top: ISOLTRAP section of the preparation Penning trap (not to scale). Retardation electrodes located in front of the trap slow down the ions delivered from the buncher. After ejection from the trap the ions are accelerated, pass a drift tube, and hit the MCP detector. Bottom: event sequence of a typical experimental cycle.

Note that the width of a resonance curve obtained from the number of detected ions as a function of the excitation frequency is influenced by the size of the diaphragm in the upper endcap of the preparation trap (see Fig. 2). By use of a straight-line approximation for the resonance curve near $\delta = 0$ applicable for $\lambda \leq 0.5$, the width $\Delta\nu_{\mathrm{dia}}$ of the resonance at the diaphragm radius $\rho_{\mathrm{dia}}$ is given by

$$\Delta\nu_{\mathrm{dia}} = \Delta\nu_{\mathrm{mag}} \frac{2\rho_{\mathrm{dia}}}{\rho_{-}(0)}. \tag{16}$$

For more realistic experimental values (e.g., $\lambda = 0.8$), the width is decreased by a smaller factor. In any case, the width is decreased by maximizing the initial magnetron radius $\rho_{-}(0)$.

## 5. Experimental results

The quality of an excitation scheme for ion separation is mainly characterized by two properties, the centering efficiency and the resolving power. The centering efficiency is defined by the ratio of the number of ions detected after the complete procedure (step *A*–*H* in Fig. 3 bottom) with resonant excitation to the number of ions when ejecting them immediately after step *D*. The resolving power is determined by an evaluation of the measured ion count as a function of the excitation frequency (so called cooling resonance). In the following the cooling-resonance shape of octupolar excitation and systematic measurements of the resolving power for both quadrupolar and octupolar excitation are presented. The parameters studied for the centering efficiency are the pressure $p_{\mathrm{read}}$ and the excitation amplitudes, $U_{\mathrm{q}}$ for quadrupolar excitation and $U_{\mathrm{oct}}$ for octupolar excitation. The parameters studied for the resolving power are the pressure $p_{\mathrm{read}}$ and the excitation durations $\tau_0$. As a further issue especially for the performance of a separation process for unstable ions, the overall duration of the process will be discussed.

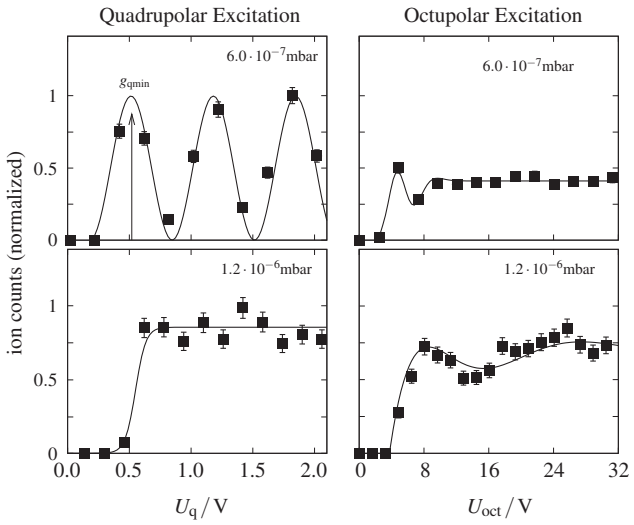


**Fig. 4.** Normalized ion count as a function of the excitation amplitude for quadrupolar (left) and octupolar (right) excitation. Pressures at the Penning gauge are (top): $6.0 \times 10^{-7}$ mbar, (bottom): $1.2 \times 10^{-6}$ mbar. Lines to guide the eye.

### 5.1. Centering efficiency

For an excitation duration of $\tau_0 = 50$ ms and two different pressures, the ion yield has been determined as a function of the excitation amplitude. The excitation frequency was set to the resonance frequency $\nu_c$ for quadrupolar excitation and $2\nu_c$ for octupolar excitation. The normalized ion count for quadrupolar (octupolar) excitation is shown in Fig. 4 left (right). For quadrupolar excitation at low pressures (top) the ion count oscillates as a function of the amplitude, since $\lambda < 1$ (see Section 3.1) for at least all amplitudes above the one corresponding to $g_{\mathrm{q_{min}}}$. For suitable amplitudes, the efficiency is typically 80–100 %. For higher pressures (bottom) the efficiency range is similar, but the ions are detected for all amplitudes above a minimum value. This means that $\lambda \geq 1$ or, in the case of higher amplitudes, $\lambda < 1$ with the corresponding oscillations of the ion count not detectable, since, due to the higher pressure, the total radius is already smaller than $\rho_{\mathrm{dia}}$ upon ejection.

Due to the asynchronous conversion in case of octupolar excitation (see Section 2), only small oscillations of the ion count have been observed even for low pressures (top). The large distribution of final radii leads to a maximum efficiency of about 50%. For $p_{\mathrm{read}} = 1.2 \times 10^{-6}$ mbar, which is commonly used in the experiment, the efficiency grows to about 75%.

### 5.2. Octupolar cooling resonances

An example of a cooling resonance for octupolar excitation of $^{133}Cs^{+}$ ions is shown in Fig. 5 top. The shapes of cooling resonances with octupolar excitation are similar to those obtained

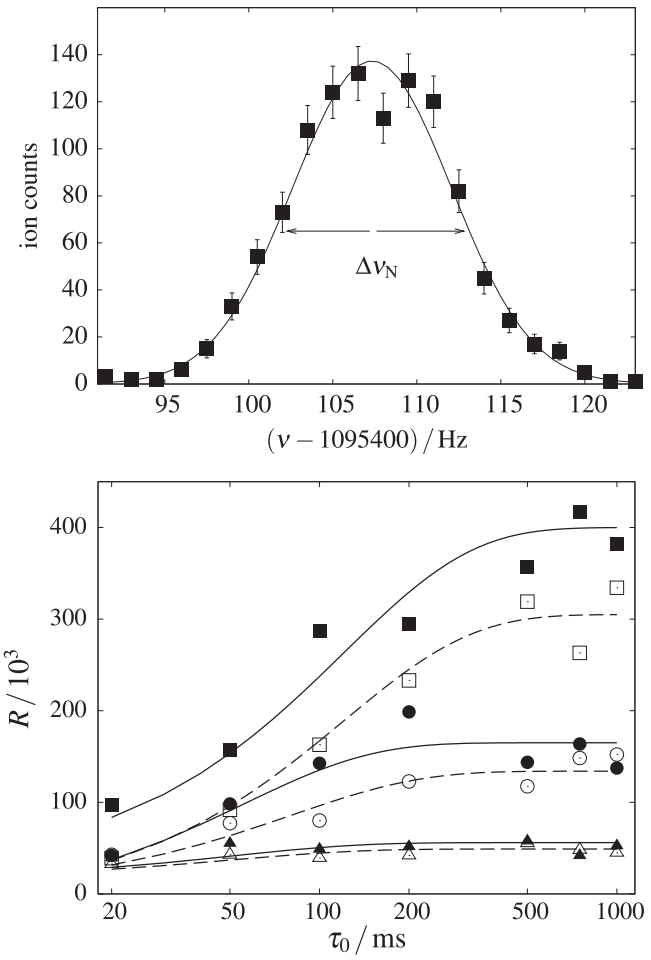


**Fig. 5.** Top: ion count as a function of the frequency for octupolar excitation for $\tau_0 = 50$ ms and a pressure of $p_{read} = 6.0 \times 10^{-7}$ mbar. Bottom: resolving power as a function of the excitation duration (logarithmic time scale) for quadrupolar excitation (open symbols) and octupolar excitation (full symbols) at a pressure of $p_{read} = 3.0 \times 10^{-7}$ mbar (squares), $p_{read} = 6.0 \times 10^{-7}$ mbar (circles), and $p_{read} = 1.2 \times 10^{-6}$ mbar (triangles) at the Penning gauge. Dashed (quadrupolar excitation) and solid lines (octupolar excitation) to guide the eye. Statistical error-bar sizes are on the order of the symbol size.

with quadrupolar excitation and have been fitted with a Gaussian [24,25]. The resolving power obtained in the experiment is determined by $R = \nu_c/\Delta\nu_N$ for quadrupolar, and $R = 2\nu_c/\Delta\nu_N$ for octupolar excitation, where $\Delta\nu_N$ is the FWHM of the ion count as a function of the frequency. For the same width $\Delta\nu_N$ for both excitation schemes, one obtains thus for octupolar excitation twice the resolving power of the quadrupolar excitation. The characteristic phase dependence of octupolar excitation disappears for typical excitation durations $\tau_0 > 20$ ms, since collisions with the buffer gas disturb the motion and the initial phase distribution averages out resulting in a larger width of the resonance curve.

### 5.3. Resolving power

The resolving power $R$ has been studied for different values of the pressure $p_{read}$ and the excitation duration $\tau_0$. In each case, the excitation amplitude has been optimized to achieve the highest resolving power (see Section 3.2).

The results for quadrupolar and octupolar excitation are shown in the bottom of Fig. 5. Systematic measurements have been performed for excitation durations ranging from 20 ms to 1000 ms at pressures of $p_{read} = 3.0 \times 10^{-7}$ mbar, $p_{read} = 6.0 \times 10^{-7}$ mbar, and $p_{read} = 1.2 \times 10^{-6}$ mbar at the Penning gauge (about $10^{-5}$ mbar to $10^{-4}$ mbar inside the trap). A significant difference in resolving power between both excitation schemes is only visible for the lowest pressure $p_{read} = 3.0 \times 10^{-7}$ mbar, where octupolar excitation shows an advantage for short excitation durations and reaches $R \approx 4 \times 10^5$ for longer excitation. Use of this pressure, however, requires long waiting times to cool the motional modes of the ions. Thus, a preparation time of 700 ms has been added to the main step of the experimental cycle (step F in Fig. 3). Also, the efficiency of octupolar excitation is below 40%. For the typical pressure of $p_{read} = 1.2 \times 10^{-6}$ mbar at the Penning gauge (additional preparation time of 400 ms), saturation for the resolving power is reached already after $\tau_0 = 100$ ms for both excitation schemes and the resolving powers are comparable.

## 6. Simulations

The measurements described above will be compared with simulations of the ion trajectories in the preparation Penning trap. To this end, a simulation program has integrated the equation of motion for test particles assuming ideal electric fields and neglecting ion–ion interactions.

Although requiring more algebraic calculations than a standard integrator like the fifth-order Runge–Kutta method, the fifth-order Gear integrator [26] was chosen because the force has to be calculated only once per time step. The repetition of the calculation of the force is more computation-time consuming than that of the integrator. Thus, the Gear integrator is quite effective. In addition, it guarantees a still admissible deviation from energy conservation.

A binary-collision model is used for collisions of the trapped particles with the buffer gas. For every time step, the probability $P$ of a collision of an ion with a buffer-gas atom is calculated as a function of the number density $n_{gas}$ of the buffer gas (determined by the pressure $p$), the velocity difference $u$ between buffer-gas atom and ion, and the cross section $\sigma$ for $^{133}Cs^+$ ions in a $^4He$ gas at room temperature, which are obtained from [27]

$$P = 1 - \exp(-un_{gas}\sigma\Delta t). \tag{17}$$

In case of a collision, the polar scattering angle $\Theta$ in the center-of-mass system is sampled from the uniform probability distribution UD according to the binary collision model inspired by Takizuka and Abe [28] and further generalized in Ref. [29],

$$\cos(\Theta) = 1 - 2(\mathrm{UD}), \tag{18}$$

where UD is a random number between 0 and 1. The azimuthal scattering angle $\Phi$ is sampled isotropically by $\Phi = 2\pi(\mathrm{UD})$.

### 6.1. Initial conditions and procedure

The ion cloud in the trap is described by a Gaussian distribution in space. To determine the initial radial bunch width $\Delta\rho$, i.e., the situation after step C in the bottom of Fig. 3, simulations of a precooling process for three typical pressures used in the trap have been performed. The initial bunch width scales from 0.5 mm for $p = 20 \times 10^{-5}$ mbar to 1.0 mm for $p = 2 \times 10^{-5}$ mbar and has been linearly interpolated for pressure values in between. For pressures below $p = 2 \times 10^{-5}$ mbar, the bunch width was assumed to remain constant, $\Delta\rho = 1.0$ mm.

An average magnetron radius of 5 mm is assumed to represent experimental conditions after step E in the bottom of Fig. 3. Then, the centering excitation is applied and the residual magnetron radius is determined. Ions with a magnetron radius smaller than the diaphragm radius $\rho_{dia}$ are counted as cooled ions assuming that the residual cyclotron radius is decreased sufficiently after a certain waiting time. The simulations have been performed for an excitation duration of $\tau_0 = 50$ ms, various coupling parameters $g = g_q$ ($g = g_{oct}$) and pressures $p$.

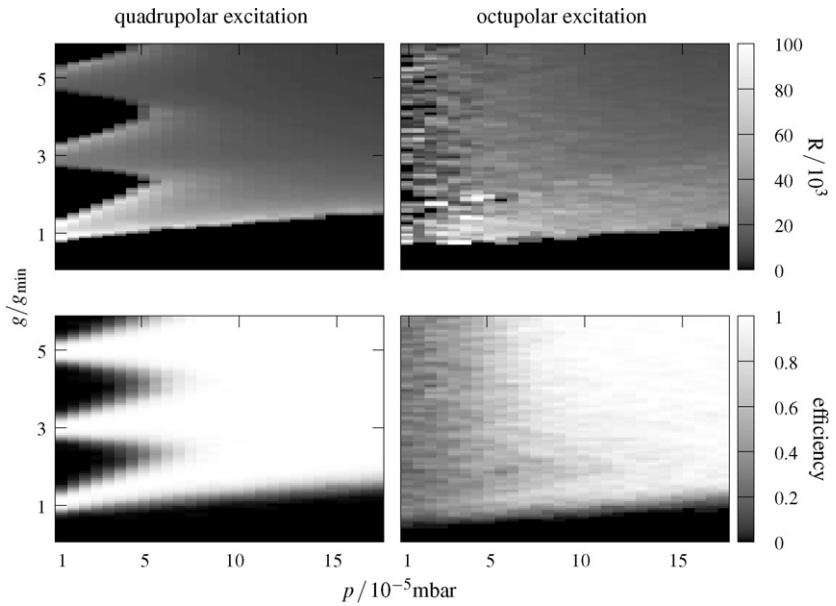


**Fig. 6.** Resolving power (top) and efficiency (bottom) of the cooling process for $^{133}Cs^+$ ions as a function of the pressure and the coupling parameter $g$ normalized to the minimum required $g_{min}$ to center the ions (i.e., $g_{min} = g_{q_{min}}$ for quadrupolar excitation with $\tau_0 = 50$ ms). Results for quadrupolar excitation (left) and octupolar excitation (right).

For each of these ($g$, $p$) parameter sets the efficiency and the resolving power $R$ have been extracted from the simulation. To calculate the resolving power, $\Delta\nu_N$ has been determined from searching the frequency where half of the ion number as compared to the simulation at the resonance frequency are in the center region. To this end the bisection method has been used in order to reduce the number of simulation steps needed for the search. The search is performed uni-directional, since also for octupolar excitation the cooling resonances are assumed to be symmetric (see Fig. 5 top).

### 6.2. Comparison of simulations with experimental results

The results of the simulation of the resolving power and the efficiency for both excitation schemes are shown in Fig. 6. The efficiency ranges from 0 (0%) to 1 (100%). Resolving powers for points with an efficiency less than 30% have not been calculated and are set to 0.

The simulation yields a maximum resolving power of $R_{max} \approx 1 \times 10^5$ for both excitation schemes. At a pressure of $p = 4.0 \times 10^{-5}$ mbar the octupolar excitation scheme reaches its maximum in resolving power and shows a slight advantage as compared to quadrupolar excitation, whereas for higher pressures the resolving powers are comparable. This agrees with the experimental findings ($\tau_0 = 50$ ms in the bottom of Fig. 5). This means that for octupolar excitation the width $\Delta\nu_N$ of the resonance is doubled as compared to quadrupolar excitation for most of the simulated pressures. The efficiency values for quadrupolar excitation show the expected results. A transition from the oscillating to the overdamped motion scheme is observed and all ions are centered for optimized amplitudes. For octupolar excitation, a loss of ions (to 50% and less) is found for low pressures, where the simulated curves reproduce the measured curves in Fig. 4 quite well, including the absence of the periodical count rate oscillations for low pressures (see Section 5.1).

The drop of the resolving power for octupolar excitation compared to the results in Refs. [12,13] is a consequence of the collisions (as illustrated in Fig. 7). The ion motion, excited by a quadrupolar excitation, is still comparable with the corresponding motion with a continuous damping coefficient $\gamma$, since small changes of the trajectories have a small influence on the conversions.

In the case of octupolar excitation, however, the ions react strongly on the collisions and the resulting new initial conditions for the next part of the simulation lead to drastic deviations from the trajectory without collisions. Thus the conversions are interrupted, which further decreases the efficiency and reduces the resolving power.

In contrast, a continuous damping ansatz of the form of Eq. (6), which has been simulated in the same way as described in Section 6.1, leads to resolving powers for octupolar excitation of up to $R_{max} \approx 10^7$ (not shown). This result is in contradiction to the experimental values. Thus, for octupolar excitation the continuous damping approach does not adequately describe the ion motion in contrast to the microscopic collision model. Further examples for the necessity of using a microscopic model instead of a continuous damping force can be found in Ref. [27], where the interaction of ions with buffer-gas atoms in RFQ devices is discussed. As also

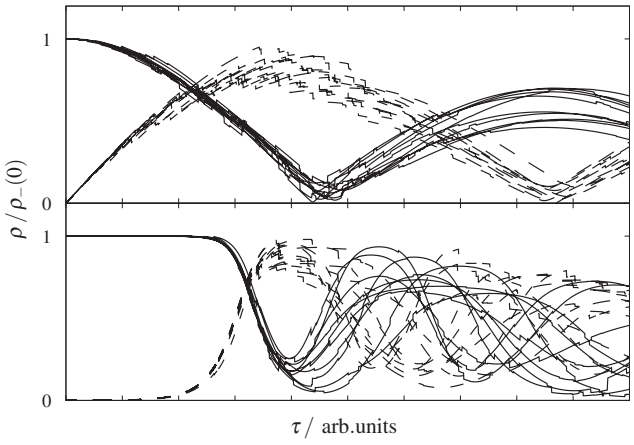


**Fig. 7.** Magnetron (solid lines) and cyclotron radii (dashed lines) of ten $^{133}Cs^+$ ions for quadrupolar excitation (top) and octupolar excitation (bottom) as a function of excitation time from a simulation including collisions. All ions have the same initial conditions.

indicated in a recent study [30] collision models have to be chosen according to their validity at different ion energies.

## 7. Summary

The application of octupolar excitation for mass-selective centering of ions in a Penning trap has been investigated by measurements at ISOLTRAP and compared to simulations. The experimental study was conducted for different pressures, excitation durations and amplitudes. For octupolar excitation, a gain in resolving power as compared to quadrupolar excitation can be obtained, but only for lower pressures than typically used in the experiment which in turn require longer experimental cycles. In addition, the efficiency of octupolar excitation decreases to below 50% for these pressures.

The experimental results have been reproduced by simulations including a binary-collision model. The decreased efficiency for octupolar excitation at low pressures is explained by the asynchronous conversions due to different initial radii.

In contrast to a continuous damping approach the binary-collision-model simulations show the non-negligible influence of the individual buffer-gas collisions on the ion motion in case of octupolar excitation. The sensitive reaction of the system explains the measured decrease in the resolving power for commonly used buffer-gas pressures as compared to collision-free resonances.

## Acknowledgments

This work was supported by the Max-Planck Society, the German Federal Ministry for Education and Research (BMBF FKZ 06GF1861 and 06GF9102). We are grateful to Prof. K. Blaum, Prof. M. Kretzschmar and Dr. S. George for valuable discussions during this work.

## References

[1] G. Savard, St. Becker, G. Bollen, H.-J. Kluge, R.B. Moore, Th. Otto, L. Schweikhard, H. Stolzenberg, U. Wiess, Phys. Lett. A 158 (1991) 247.
[2] K. Blaum, Phys. Rep. 425 (2006) 1.
[3] L. Schweikhard, G. Bollen (Eds.), Int. J. Mass Spectrom. 251 (2006) (special issue).
[4] L. Schweikhard, S. Guan, A.G. Marshall, Int. J. Mass Spectrom. Ion Process. 120 (1992) 71.
[5] S. Guan, H.S. Kim, A.G. Marshall, M.C. Wahl, T.D. Wood, X. Xiang, Chem. Rev. 94 (8) (1994) 2161.
[6] P.B. O'Connor, J.P. Speir, T.D. Wood, R.A. Chorush, Z. Guan, F.W. McLafferty, J. Mass Spectrom. 31 (5) (1996) 555.
[7] Ch. Weber, G. Audi, D. Beck, K. Blaum, G. Bollen, F. Herfurth, A. Kellerbauer, H.-J. Kluge, D. Lunney, S. Schwarz, Phys. Lett. A 347 (2005) 81.
[8] J. Van Roosbroeck, C. Guenaut, G. Audi, D. Beck, K. Blaum, G. Bollen, J. Cederkall, P. Delahaye, H. De Witte, D. Fedorov, V.N. Fedoseyev, S. Franchoo, H. Fynbo, M. Gorska, F. Herfurth, K. Heyde, M. Huyse, A. Kellerbauer, H.-J. Kluge, U. Koster, K. Kruglov, D. Lunney, A. De Maesschalck, V.I. Mishin, W.F. Mueller, S. Nagy, S. Schwarz, L. Schweikhard, N.A. Smirnova, K. Van de Vel, P. Van Duppen, A. Van Dyck, W.B. Walters, L. Weissmann, C. Yazidjian, Phys. Rev. Lett. 92 (2004) 112501.
[9] S. George, S. Baruah, B. Blank, K. Blaum, M. Breitenfeldt, U. Hager, F. Herfurth, A. Herlert, A. Kellerbauer, H.-J. Kluge, M. Kretzschmar, D. Lunney, R. Savreux, S. Schwarz, L. Schweikhard, C. Yazidjian, Phys. Rev. Lett. 98 (2007) 162501.
[10] S. George, K. Blaum, F. Herfurth, A. Herlert, M. Kretzschmar, S. Nagy, S. Schwarz, L. Schweikhard, C. Yazidjian, Int. J. Mass Spectrom. 264 (2007) 110.
[11] T. Eronen, V.-V. Elomaa, U. Hager, J. Hakala, A. Jokinen, A. Kankainen, S. Rahaman, J. Rissanen, C. Weber, J. Aysto, Nucl. Instrum. Methods B 266 (2008) 4527.
[12] R. Ringle, G. Bollen, P. Schury, S. Schwarz, T. Sun, Int. J. Mass Spectrom. 262 (2007) 33.
[13] S. Eliseev, M. Block, A. Chaudhuri, F. Herfurth, H.-J. Kluge, A. Martin, C. Rauth, G. Vorobjev, Int. J. Mass Spectrom. 262 (2007) 45.
[14] M. Breitenfeldt, F. Ziegler, A. Herlert, G. Marx, L. Schweikhard, Int. J. Mass Spectrom. 263 (2007) 94.
[15] S. Eliseev, C. Roux, K. Blaum, M. Block, C. Droese, F. Herfurth, M. Kretzschmar, M.I. Krivoruchenko, E. Minaya Ramirez, Yu.N. Novikov, L. Schweikhard, V.M. Shabaev, F. Šimkovic, I.I. Tupitsyn, K. Zuber, N.A. Zubova, Phys. Rev. Lett. 107 (2011) 152501.
[16] L.S. Brown, G. Gabrielse, Rev. Mod. Phys. 58 (1986) 233.
[17] F.G. Major, V.N. Gheorghe, G. Werth, Charged Particle Traps, in: Physics and Techniques of Charged Particle Field Confinement (Springer Series on Atomic, Optical, and Plasma Physics, vol. 37), Springer-Verlag, Berlin, 2005.
[18] M. König, G. Bollen, H.J. Kluge, T. Otto, J. Szerypo, Int. J. Mass Spectrom. 142 (1995) 95.
[19] S. George, K. Blaum, M. Block, M. Breitenfeldt, M. Dworschak, F. Herfurth, A. Herlert, M. Kowalska, M. Kretzschmar, E. Minaya Ramirez, D. Neidherr, S. Schwarz, L. Schweikhard, Int. J. Mass Spectrom. 299 (2011) 102.
[20] E.A. Mason, E.W. McDaniel, Transport Properties of Ions in Gases, John Wiley and Sons, New York, 1988.
[21] G. Bollen, R.B. Moore, G. Savard, H. Stolzenberg, J. Appl. Phys. 68 (1990) 4355.
[22] M. Mukherjee, D. Beck, K. Blaum, G. Bollen, J. Dilling, S. George, F. Herfurth, A. Herlert, A. Kellerbauer, H.J. Kluge, S. Schwarz, L. Schweikhard, C. Yazidjian, Eur. Phys. J. A 35 (2008) 1.
[23] F. Herfurth, J. Dilling, A. Kellerbauer, G. Bollen, S. Henry, H.-J. Kluge, E. Lamour, D. Lunney, R.B. Moore, C. Scheidenberger, S. Schwarz, G. Sikler, J. Szerypo, Nucl. Instrum. Methods A 469 (2001) 254.
[24] V.S. Kolhinen, S. Kopecky, T. Eronen, U. Hager, J. Hakala, J. Huikari, A. Jokinen, A. Nieminen, S. Rinta-Antila, J. Szerypo, J. Äystö, Nucl. Instrum. Methods A 528 (2004) 776.
[25] S. Rahaman, M. Block, D. Ackermann, D. Beck, A. Chaudhuri, S. Eliseev, H. Geissel, D. Habs, F. Herfurth, F.P. Heßberger, S. Hofmann, G. Marx, M. Mukherjee, J.B. Neumayr, M. Petrick, W.R. Plaß, W. Quint, C. Rauth, D. Rodríguez, C. Scheidenberger, L. Schweikhard, P.G. Thirolf, C. Weber, Int. J. Mass Spectrom. 251 (2006) 146.
[26] C.W. Gear, Numerical Initial Value Problems in Ordinary Differential Equations, Prentice Hall PTR, Upper Saddle River, NJ, USA, 1971.
[27] S. Schwarz, Simulations for ion traps - buffer gas cooling in trapped charged particles and fundamental interactions, in: K. Blaum, F. Herfurth (Eds.), Lecture Notes in Physics, vol. 749, Springer-Verlag, Berlin, Heidelberg, 2008.
[28] T. Takizuka, H. Abe, J. Comp. Phys. 25 (1977) 205.
[29] K. Matyash, Phd. Thesis at Ernst-Moritz-Arndt-Universität Greifswald (2003).
[30] Z.C. Zhu, W.X. Huang, Y.L. Sun, Y. Wang, Y.L. Tian, J.Y. Wang, Int. J. Mass Spectrom. 309 (2012) 44.